Geol. Mag. **152** (*6*), *2015, pp. 957–972.* © *Cambridge University Press 2015*
doi:10.1017/S0016756814000818

Sourceland controls and dispersal pathways of Holocene muds from boreholes of the Ionian Basin, Calabria, southern Italy

FRANCESCO PERRI†, SALVATORE CRITELLI, ROCCO DOMINICI, FRANCESCO MUTO & MAURIZIO PONTE

Dipartimento di Biologia, Ecologia e Scienze della Terra, Università degli Studi della Calabria, Via P. Bucci, 87036 Arcavacata di Rende (CS), Italy

(*Received* 30 June 2014; *accepted* 15 December 2014; *first published online* 11 February 2015)

Abstract – Deep-marine muds were collected from two boreholes (Crati II and Neto VI) along the Ionian Calabrian Basin. The samples from the Crati II and the Neto VI boreholes show a similar mineralogical distribution; the marine muds contain mostly phyllosilicates, quartz, calcite, feldspars and dolomite. Traces of gypsum are present in a few samples. The Neto muds show higher concentrations of carbonates than the Crati muds; these contents are mainly related to recycling of the Neogene–Quaternary carbonate-rich marine deposits of the Crotone Basin, which mostly influences the composition of the Neto muds. The geochemical signatures of the muds mainly reflect a provenance characterized by felsic rocks with a minor, but not negligible, mafic supply. In particular, the hinterland composition of the Crati drainage area is on average more mafic in composition than the Neto drainage area. The higher mafic concentration of the Crati sample muds is probably related to the ophiolitiferous units that are exposed in the Crati drainage basin. The degree of source area weathering was most probably of low–moderate intensity because the Chemical Index of Alteration values for the studied muds range from 67 to 69. Furthermore, the low and constant Al/K and Rb/K ratios suggest low–moderate weathering without important fluctuations in weathering intensity. The Al_2O_3–TiO_2–Zr ternary diagram and the values of the Index of Compositional Variability indicate that both the Neto and Crati muds are first-cycle, compositionally immature sediments, related to a tectonically active (collision) setting such as the Calabria–Peloritani Arc, where chemical weathering plays a minor role.

Keywords: Ionian Basin, northeastern Calabria, mineralogical distribution, geochemical signature, provenance.

1. Introduction

The Calabrian Arc is an arcuate terrane composed of a pile of pre-Mesozoic polymetamorphic nappes comprising large sheets of Hercynian crystalline basement (forming the Sila and Aspromonte massifs) and local remnants of a Mesozoic to Cenozoic succession, that separates the Ionian and Tyrrhenian basins connecting the NW-trending southern Apennine chain and the E-trending Sicilian Maghrebides (e.g. Bonardi *et al.* 2001; Critelli *et al.* 2013; Tripodi, Muto & Critelli, 2013).

The Calabrian Arc migrated southeastwards from mid-Miocene time onwards in response to the subduction of the Ionian oceanic lithosphere along a deep and narrow W-dipping Benioff zone (among others Bonardi *et al.* 2001; Speranza *et al.* 2012; Zecchin *et al.* 2013 and references therein); this movement caused a fragmentation of the arc into individual blocks bounded by NW-trending shear zones, which controlled the development of basins located along both the Ionian and Tyrrhenian sides of Calabria (Knott & Turco, 1991).

Among the streams that drain the northern portion of the Calabrian Arc, the Crati and Neto rivers are the main drainage systems connecting the terrestrial source areas to the marine deposits within the peri-Ionian Basin. The main entry points for sediment into the Ionian Basin include several canyons and gullies. Fluvial sediment input is dominant for the entire borderland, whereas biogenic and aeolian inputs are minor. The western portions of the Taranto Gulf are dominated by the Crati Submarine Fan, the largest fan in the northern part of the study area. The Neto River is the most important drainage system of the southern area, which feeds into the Ionian deep Basin through the Neto Canyon to the north of the Luna–Hera Lacinia structural high (e.g. Le Pera *et al.* 2001; Rebesco *et al.* 2009; Zecchin *et al.* 2011; Critelli *et al.* 2012; Perri *et al.* 2012*b*).

During the last three decades many explorations of the seafloor have illustrated the widespread occurrence of submarine depositional systems. The sedimentary fill of basins is related to several factors based on relationships between source areas and depositional environment. The use of sediment geochemistry and its combination with mineralogical analyses of marine muds represents an important tool for the investigation of the processes that occurred from sediment generation on the uplands to the final accommodation on the bathyal plain. In particular, the distribution of major and trace elements, obtained by X-ray fluorescence spectrometry (XRF), related to the mineralogical variations, deduced

†Author for correspondence: francesco.perri@unical.it

from the evolution of the X-ray diffraction (XRD) patterns, of fine-grained sediments is widely used to explain and reconstruct the source area composition and the weathering and diagenetic processes (e.g. Bauluz *et al.* 2000; Perri *et al.* 2008, 2011, 2013; Mongelli *et al.* 2006; Critelli *et al.* 2008; Zaghloul *et al.* 2010).

The present paper represents a good opportunity to study continental weathering, sediment generation and the depositional processes in the northern Calabrian Ionian Basin through the use of chemical and mineralogical variations in marine muds sampled along the Crati II and Neto VI boreholes.

2. Regional geology

The northern sector of the Calabrian Arc is characterized from west to east by the Coastal Chain and Sila Massif and is separated by a large transversal depression formed in Plio-Pleistocene times (Catanzaro Graben) from the southern sector (e.g. Bonardi *et al.* 2001 and many others). To the southeast, the Calabrian Arc is delimited by the Ionian subduction zone (Rossi & Sartori 1981), where the Ionian lithosphere is subducted northwestward underneath the Calabrian Arc (e.g. Cavazza & Ingersoll, 2005).

The Taranto Gulf is located offshore along the coast of southern Italy between Calabria and Puglia and it characterizes the northwestern portion of the Ionian Sea. The western portion of the Taranto Gulf along the Calabrian margin displays a complex morphology consisting of ridges and basins related to the Neogene–Quaternary geodynamic evolution of the submerged, tectonically active extremity of the southern Apennines (Romagnoli & Gabbianelli, 1990; Zecchin *et al.* 2011; Perri *et al.* 2012*b*; Ceramicola *et al.* 2014). Major NW-SE and minor NE–SW-trending regional faults determine the structural evolution of this area (Romagnoli & Gabbianelli, 1990; Van Dijk *et al.* 2000).

The most important submarine fan of the northern Ionian Basin is the Crati Fan; other smaller fans close to the mouth of the Neto River, developed during Holocene time and connected with the torrential-type deltas on the shelf, further characterize this portion of the Ionian Basin along the Calabrian coast. These fans are related to the developed fluvial systems, the Crati and Neto rivers, and diverse smaller coastal rivers draining both the Calabrian continental block (i.e. Sila Massif) and the southern Apennines thrust belt (i.e. Pollino Massif); in particular, the drainage systems belonging to the Crati River drain both the Calabrian crustal block and the Mesozoic to Tertiary sedimentary terranes of the southern Apennines.

The Sila Massif is composed of plutonic–metamorphic rocks with subordinate sedimentary source rocks producing quartzofeldspathic sand, which characterize its sedimentary cover (e.g. Critelli & Le Pera, 1998, 2003; Le Pera *et al.* 2001; Barone *et al.* 2008; Critelli *et al.* 2013). To the north, the Pollino Massif is an additional source of sediments composed of sedimenticlastic sand reflecting a multi-cycle provenance from siliciclastic and carbonate strata of the platform-basin tectonostratigraphic units, such as the Cilento Group and younger sequences (e.g. Perri *et al.* 2012*c*; Critelli *et al.* 2013 and references therein). Submarine structural highs, such as the Amendolara embankment which borders the Corigliano Basin and produces reworked intrabasinal carbonate detritus (e.g. Critelli *et al.* 2007), and a series of Pleistocene terraces along the promontory of Capo Colonna enriched in carbonate strata, constitute additional sources of Quaternary sediment for the Ionian Basin margin (e.g. Zecchin *et al.* 2011 and references therein).

2.a. Crati and Neto drainage systems

Sediments in the northern portion of the Ionian Basin are mainly supplied by the Crati River and many small coastal drainage systems such as the Trionto and Saraceno Fiumara rivers. The Crati River occupies the eastern sector of the Crati Basin, which is bounded by NW–SE-trending left-slip faults (Van Dijk *et al.* 2000); the Crati Basin further collects all the small streams that drain the Coastal Range to the west and the Sila Massif to the east. Among the small streams, the Saraceno Fiumara drains the Pollino Massif and reflects a multicycle provenance from siliciclastic and carbonate strata of the Panormide, Liguride and Sicilide complexes, as well as the Cilento Group and younger sequences. The Trionto River drains the northeastern sector of the Sila Massif, which is composed of low- to medium–high-grade metamorphic rocks intruded by plutonic rocks ('granitoids' of the Sila Batholith) with a sedimentary cover (Longobucco Group), and the Miocene–Pleistocene sedimentary successions of the northern Ionian coast (e.g. Barone *et al.* 2008; Corbi *et al.* 2009; Robustelli *et al.* 2009) (Fig. 1).

Sediments in the southern portion of the Ionian Basin are mainly supplied by the Neto River and many small coastal drainage systems. The high Neto drainage system is mainly constituted by highly weathered gneiss and plutonic rocks of the Sila Unit (e.g. Scarciglia, Le Pera & Critelli, 2007), phyllites and micaschist, and Mesozoic sedimentary cover (Longobucco Group). The lower source area is chiefly composed of conglomerate, sandstone, calcarenite, marl and clay, and minor evaporites (gypsarenite, carbonate and halite) of Neogene–Quaternary age (e.g. Lugli *et al.* 2007; Perri, Dominici & Critelli, 2014).

3. Sampling and methods

Samples analysed in this study are collected from two different boreholes (Neto and Crati boreholes) that were cored through the seabed sediments of the northern Ionian Basin (Fig. 1) on board R/V OGS-Explora during the western Gulf of Taranto (WGDT) cruise (21 August – 1 September 2005). The Crati borehole is approximately 200 cm in length with a diameter of 12 cm; the Neto borehole is approximately 180 cm in length with a diameter of 12 cm. Subsampling was

https://doi.org/10.1017/S0016756814000818 Published online by Cambridge University Press

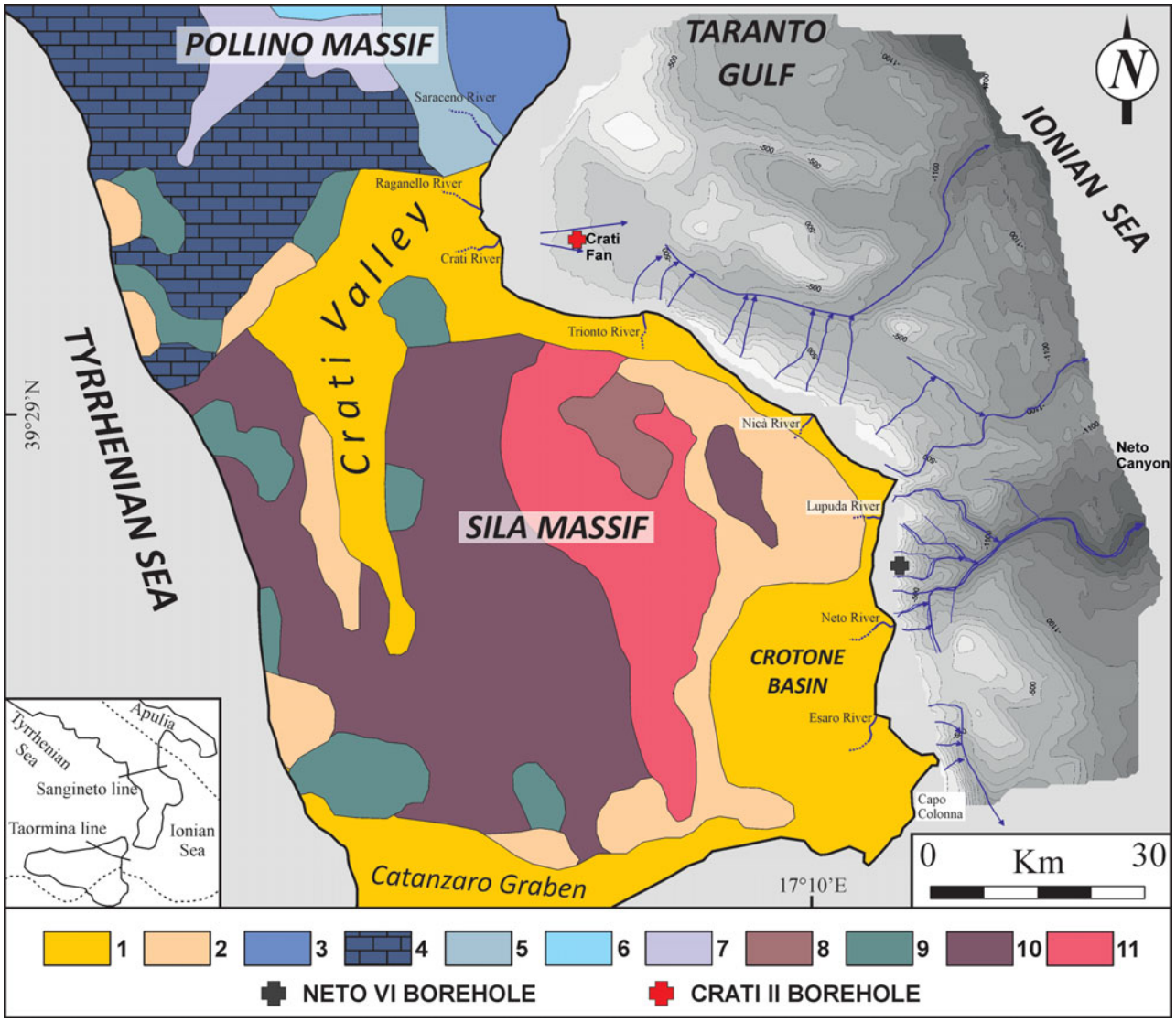

Figure 1. (Colour online) Geological sketch map of the northern sector of the Calabria–Peloritani Arc and the investigated area in the northern Ionian Basin (Taranto Gulf). The positions of the Crati II and Neto VI boreholes are also shown. 1 – Sedimentary rocks (Pliocene to Holocene); 2 – clastic rocks and evaporites (Serravallian to Messinian); 3 – Cilento Group (Middle Miocene); 4 – Apennine units of the Pollino Massif (Triassic to Miocene); 5 to 7 – Liguride Complex: 5 – Calabro–Lucanian Flysch Unit (Upper Jurassic to Upper Oligocene); 6 – Ophiolitiferous blocks and melange; 7 – Frido Unit (Upper Jurassic to Upper Oligocene); 8 – Longobucco and Caloveto Groups (Lower Lias to Lower Cretaceous) and Paludi Formation (Upper Oligocene); 9 – Malvito, Diamante–Terranova and Gimigliano ophiolitiferous units (Upper Jurassic to Lower Cretaceous); 10 – Sila, Castagna and Bagni basement units (Palaeozoic); 11 – plutonic rocks (Sila Batholith, Palaeozoic). Modified from Critelli *et al.* (2013), Perri *et al.* (2008) and Perri *et al.* (2012*b*).

carried out at intervals of 10 cm. Based on the grain-size analyses of these 38 samples (20 samples from the Crati borehole and 18 samples from the Neto borehole), it is possible to classify these sediments as muds (Fig. 2). In particular, the Neto muds are coarser than the Crati muds (Fig. 2). The bulk samples were crushed and milled in an agate mill to a very fine powder; the powder was successively placed in an ultrasonic bath at low power for a few minutes for disaggregation. The mineralogy was obtained by XRD using a Bruker D8 Advance diffractometer (CuKα radiation, graphite secondary monochromator, sample spinner; step size 0.02; speed 1 sec for step) at the Università della Calabria (Italy). Semiquantitative mineralogical analysis of the bulk rock was carried out on random powders measuring the principal peak areas using the WINFIT computer program (Krumm, 1996), according to the methods proposed by Cavalcante *et al.* (2007), Perri (2008), Perri, Muto & Belviso (2011) and Perri *et al.* (2012*a*).

Elemental analyses for major and some trace elements (Nb, Zr, Y, Sr, Rb, Ba, Ni, Co, Cr, V) were obtained by X-ray fluorescence spectrometry (XRF) using a Bruker S8 Tiger spectrometer at the Università della Calabria (Italy), on pressed powder discs of whole-rock samples, and compared to international standard-rock analyses of the United States Geological Survey. The estimated precision and accuracy for trace-element

https://doi.org/10.1017/S0016756814000818 Published online by Cambridge University Press

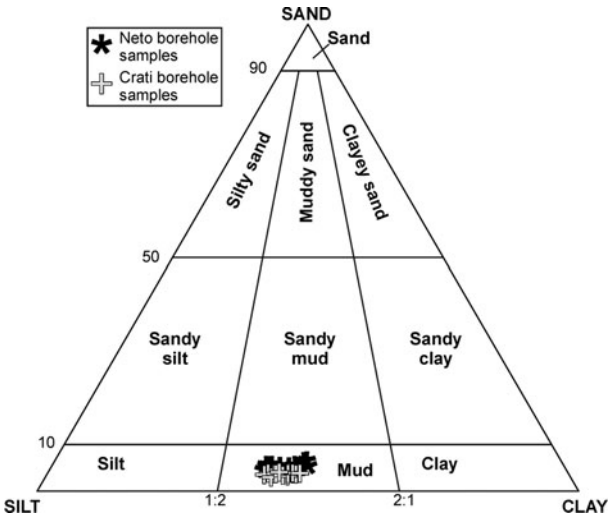

Figure 2. Sand–silt–clay ternary diagram of the studied samples from the Neto and Crati boreholes.

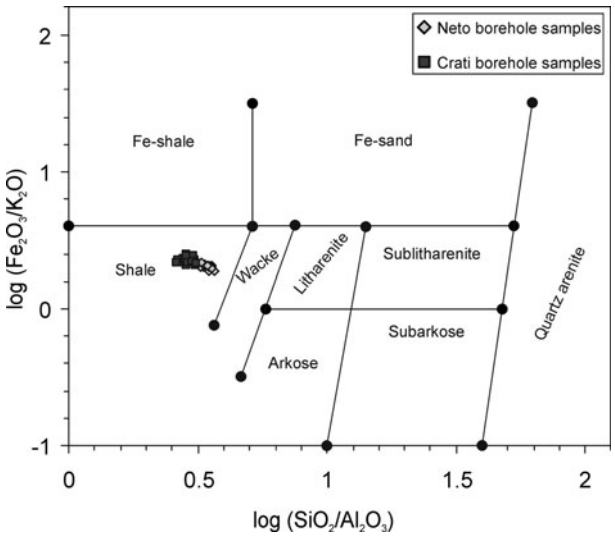

Figure 3. Chemical classification of the samples from the Neto and Crati boreholes, based on the $\log(SiO_2/Al_2O_3)$ v. $\log(Fe_2O_3/K_2O)$ diagram of Herron (1988).

determinations are better than 5 %, except for those elements having a concentration of 10 ppm or less (10–15 %) (e.g. Mongelli *et al.* 2006). Total loss on ignition (LOI) was determined after heating the samples for three hours at 900 °C.

In this study, the log-ratio-transformed composition data were used, in order to undertake normal statistical tests and express the results graphically on the Real sample space (Aitchison, 1986). Statistical confidence regions and compositional linear trends on the ternary diagrams were depicted following the methods of Weltje (2002) and von Eynatten (2004).

4. Results

4.a. Mineralogy of marine mud

The Crati and Neto borehole samples are mainly composed of phyllosilicates as the main mineralogical components, ranging from 51 % to 56 % for the Crati samples and from 40 % to 44 % for the Neto samples (Table 1). Quartz, carbonate minerals (calcite and dolomite) and feldspars (plagioclase and K-feldspar) represent the non-phyllosilicate minerals for both borehole samples. Traces of gypsum are contained in a few samples. Quartz ranges from 29 % to 32 % for the Crati samples and from 33 % to 36 % for the Neto samples. K-feldspar has a lower concentration in the Crati samples than in the Neto samples, whereas plagioclase is present in equal percentages with values up to 6 %. Calcite has a higher concentration in the Neto samples than the Crati samples, whereas dolomite is present in equal percentages with values up to 3 %. Variation in mineral concentrations is mainly related to the different source areas that influence the mineralogical compositions of the studied muds. The < 2 μm grain-size fraction is mainly composed of 10 Å-minerals (illite and micas) and chlorite for both the Crati and Neto samples. Mixed-layer clay minerals and kaolinite contents are usually low and in equal percentages.

4.b. Whole-rock geochemistry of marine muds

Major- and trace-element concentrations of the Neto and Crati borehole samples are listed in Table 2 and Table 3, respectively. The studied muds are classified using the diagram for clastic rocks (Herron, 1988). In this diagram, the SiO_2/Al_2O_3 ratio is the most commonly used parameter to characterize the clastic rock, reflecting the relative abundance of quartz, feldspar and clay minerals (e.g. Potter, 1978). The Crati samples are close to the Neto samples and plot in the field of shale indicating variation in the mica/quartz–feldspar ratio in the studied samples (Fig. 3), as shown in the mineralogical and grain-size analyses (e.g. Fig. 2).

Geochemical compositions of the Crati and Neto borehole samples were normalized to the Global Subducting Sediment (GLOSS; Plank & Langmuir, 1998), an international standard for marine sediments. This standard is dominated by terrigenous material, and therefore similar to the upper continental crust (UCC; McLennan, Taylor & Hemming, 2006) in composition (Plank & Langmuir, 1998). The general trends of the Neto (Fig. 4a, c) muds show similar variations to those of the Crati (Fig. 4b, d) muds. The studied samples are characterized by depletion in Si, Mn, Na and P, and enrichment in Ti, Al, Fe, Mg, Ca and K relative to the GLOSS (Fig. 4). Among the trace elements, the muds are enriched in the high-field-strength elements (HFSE), such as the LREEs (light rare earth elements; e.g. La and Ce), Nb and Zr, and in Cr, V and Rb, whereas they are depleted in Ni, Co and Ba relative to the GLOSS; Y and Sr show similar concentrations relative to the GLOSS (Fig. 4). Nevertheless, the Crati

https://doi.org/10.1017/S0016756814000818 Published online by Cambridge University Press

Table 1. Results of whole-rock mineralogical analyses for the studied samples from the Neto and Crati boreholes

Samples	M-L cl	Illite - micas	Chl	Kln	Σ Phyll	Qtz	K-feld	Plg	Calc	Dolom	Gyp	Σ Feld
C10	6	29	14	5	54	29	2	4	9	2	tr	6
C20	6	30	13	5	54	29	2	4	8	3	tr	6
C30	5	30	12	5	52	30	2	5	8	3	0	7
C40	5	30	11	5	51	30	2	5	10	2	0	7
C50	6	29	12	6	53	29	2	4	9	3	0	6
C60	6	31	11	5	53	29	2	4	10	2	0	6
C70	6	30	11	5	52	29	2	5	10	2	0	7
C80	5	30	12	5	52	29	2	4	11	2	0	6
C90	5	30	11	5	51	29	2	5	11	2	0	7
C100	6	29	11	5	51	29	2	6	10	2	0	8
C110	5	30	12	5	52	29	2	5	10	2	0	7
C120	5	29	12	5	51	31	2	4	10	2	0	6
C130	5	30	14	5	54	30	2	5	7	2	0	7
C140	6	29	13	5	53	32	2	4	8	1	0	6
C150	5	30	11	5	51	30	3	6	9	1	0	9
C160	6	30	14	6	56	29	2	5	7	1	0	7
C170	6	29	13	6	54	31	2	4	7	2	0	6
C180	5	30	12	5	52	31	3	5	7	2	0	8
C190	6	31	13	6	56	29	2	4	8	1	0	6
C200	5	31	12	6	54	29	2	4	8	2	0	6
N10	7	23	8	3	41	36	5	5	11	2	tr	10
N20	6	24	8	4	42	36	4	5	11	2	tr	9
N30	7	23	9	4	43	34	4	6	11	2	0	10
N40	7	24	8	5	44	33	4	5	12	2	0	9
N50	5	25	8	4	42	33	4	6	13	2	0	10
N60	6	24	8	5	43	34	4	5	12	2	0	9
N70	7	23	8	4	42	34	5	4	13	2	0	9
N80	7	22	8	4	41	33	6	5	12	3	0	11
N90	7	22	8	3	40	33	7	5	13	2	0	12
N100	5	23	9	4	41	33	5	5	13	3	0	10
N110	7	22	8	3	40	34	5	5	13	3	0	10
N120	7	22	9	3	41	35	4	6	12	2	0	10
N130	6	23	8	3	40	36	5	5	12	2	0	10
N140	6	23	8	4	41	33	5	6	12	3	0	11
N150	6	23	8	4	41	33	6	6	12	2	0	12
N160	5	25	8	5	43	36	4	4	12	1	0	8
N170	7	24	9	4	44	35	4	4	11	2	0	8
N180	5	25	9	5	44	36	4	4	11	1	0	8

Legend: M-L cl – mixed-layer clay minerals (e.g. illite–smectite, chlorite–smectite and vermiculite–smectite mixed layers); Kln – kaolinite; Phyll – sum of phyllosilicates; Qtz – quartz; Plg – plagioclase; K-Feld – K-feldspar; Calc – calcite; Dolom – dolomite; Gyp – gypsum; Feld – sum of feldspars.

muds show marked variations in elemental distribution compared to the Neto muds.

The Crati muds show a weak positive correlation between $\ln(Al_2O_3/Nb)$ and $\ln(CaO/Nb)$ and a non-correlation for the Neto muds (Fig. 5). In fine-grained sediments Al_2O_3 monitors clays (Crichton & Condie, 1993), and this trend may thus account for the competition between mica-like clay minerals and carbonates (e.g. calcite); it also suggests that the Neto samples are relatively richer in carbonates than the Crati samples. The Crati and Neto muds further show positive correlation among $\ln(Al_2O_3/Nb)$ with $\ln(TiO_2/Nb)$, $\ln(Na_2O/Nb)$, $\ln(MgO/Nb)$, $\ln(K_2O/Nb)$ and $\ln(Fe_2O_3/Nb)$ (Fig. 5), suggesting that these elements are mostly controlled by the mica-like clay minerals, and are hosted as cations mainly in the structures of chlorite and 2:1 clay minerals (illite and mixed-layer clays) (e.g. Mongelli *et al.* 2006). Clay's control on element abundances is also evident from the K_2O–Fe_2O_3–Al_2O_3 ternary diagram (e.g. Wronkiewicz & Condie, 1987) where the studied samples plot along a trend defined by chlorite and muscovite–illite end-members (Fig. 6).

5. Discussion

5.a. Source area(s) weathering, sorting and recycling conditions

Chemical weathering strongly affects major-element geochemistry and mineralogical composition of fine-grained sediments (e.g. Nesbitt & Young, 1982; Perri & Otha, 2014; Perri *et al.* 2014 and references therein). Among the weathering indices, the Chemical Index of Alteration (CIA; Nesbitt & Young, 1982) is the most useful to quantify the chemical alteration of source rocks. Since the studied sediments show high CaO values, the CIA′ index (e.g. Perri *et al.* 2014; Perri, Dominici & Critelli, 2014) expressed as molar volumes of $(Al/(Al + Na + K)) \times 100$ and, thus, calculated without the CaO content, has also been used to evaluate the source area(s) weathering. The marine muds fall in the A–CN–K and A–N–K diagrams (Fig. 7) between the feldspar join and the illite–muscovite field and show uniform CIA (on average 62 ± 0.4 for the Neto samples and 64 ± 0.8 for the Crati samples) and CIA′ (on average 68 ± 0.6 for the Neto samples and 70 ± 0.6 for the Crati samples) values reflecting low–moderate

https://doi.org/10.1017/S0016756814000818 Published online by Cambridge University Press

Table 2. Major- and trace-element concentrations and ratios for the studied samples from the Neto borehole

Samples	N10	N20	N30	N40	N50	N60	N70	N80	N90
Oxides (wt %)									
SiO_2	47.84	45.64	47.65	49.25	48.03	48.65	48.59	48.21	48.15
TiO_2	0.72	0.69	0.74	0.70	0.73	0.72	0.71	0.71	0.72
Al_2O_3	14.29	13.44	14.49	13.92	14.01	14.17	13.86	14.02	13.72
Fe_2O_3	5.88	5.62	6.12	5.58	5.94	5.81	5.73	5.62	5.86
MnO	0.08	0.09	0.09	0.08	0.09	0.08	0.08	0.08	0.09
MgO	3.12	2.99	3.17	3.06	3.16	3.13	3.13	3.08	3.11
CaO	8.27	8.27	8.29	8.50	9.19	8.57	8.75	8.57	9.23
Na_2O	1.42	1.26	1.29	1.38	1.38	1.39	1.37	1.39	1.41
K_2O	2.84	2.70	2.91	2.84	2.86	2.85	2.82	2.93	2.84
P_2O_5	0.15	0.15	0.16	0.15	0.16	0.16	0.16	0.15	0.15
LOI	14.56	18.66	14.64	13.84	13.85	13.90	14.34	14.35	14.44
Tot.	99.17	99.51	99.55	99.30	99.40	99.43	99.54	99.11	99.72
Trace elements (ppm)									
Ni	48	41	48	38	46	43	43	42	40
Cr	108	104	111	100	110	105	104	105	107
V	145	142	146	135	142	139	139	139	138
Co	15	16	17	16	14	16	16	17	15
Cu	26	22	27	21	24	25	23	21	24
Zn	119	118	127	118	119	118	124	127	114
Nb	16	16	16	16	16	15	16	15	15
Ba	405	396	398	401	385	398	400	421	383
Rb	153	151	156	149	152	153	150	157	146
Sr	348	365	355	352	384	358	372	366	384
Y	31	32	33	31	31	31	30	32	31
Zr	165	169	166	173	161	171	175	176	177
La	42	34	38	37	37	50	32	39	39
Ce	79	73	82	73	75	73	72	69	69
Ratios									
CIA	63	62	63	62	62	62	62	62	62
CIA′	69	69	70	69	69	69	69	68	68
ICV	1.56	1.60	1.55	1.58	1.66	1.59	1.62	1.59	1.69
Samples	N100	N110	N120	N130	N140	N150	N160	N170	N180
Oxides (wt %)									
SiO_2	49.37	48.53	47.75	47.69	46.95	46.64	47.53	48.45	47.24
TiO_2	0.71	0.68	0.71	0.72	0.73	0.74	0.76	0.75	0.76
Al_2O_3	14.06	13.49	13.80	13.99	14.09	14.02	14.78	14.74	14.75
Fe_2O_3	5.75	5.36	5.83	5.84	6.01	6.09	6.11	6.11	6.15
MnO	0.08	0.08	0.08	0.08	0.08	0.08	0.08	0.09	0.09
MgO	3.21	3.05	3.11	3.16	3.17	3.18	3.18	3.15	3.19
CaO	9.11	9.02	8.47	8.58	8.53	8.48	7.89	7.83	7.87
Na_2O	1.51	1.42	1.48	1.44	1.56	1.65	1.55	1.61	1.78
K_2O	2.87	2.79	2.81	2.83	2.84	2.94	3.04	3.00	3.05
P_2O_5	0.16	0.16	0.16	0.17	0.15	0.15	0.15	0.16	0.15
LOI	13.12	14.61	14.98	14.99	15.80	15.28	14.81	13.50	14.27
Tot.	99.95	99.19	99.18	99.49	99.91	99.25	99.88	99.39	99.30
Trace elements (ppm)									
Ni	39	39	40	42	45	44	46	45	45
Cr	109	100	106	104	115	106	103	108	108
V	139	129	138	138	151	146	144	143	147
Co	15	13	16	17	16	16	19	17	17
Cu	22	22	25	26	25	28	28	27	27
Zn	115	109	138	148	133	131	117	126	126
Nb	15	15	16	15	16	17	16	16	17
Ba	389	399	407	424	374	416	449	423	426
Rb	146	142	149	152	153	155	159	158	161
Sr	384	379	352	369	366	369	325	326	336
Y	32	31	31	32	31	32	33	33	33
Zr	172	186	172	171	154	167	175	174	169
La	41	37	48	39	38	41	40	45	41
Ce	66	65	74	79	79	80	80	85	84
Ratios									
CIA	63	62	62	62	62	62	62	62	61
CIA′	68	68	68	68	68	67	68	68	67
ICV	1.65	1.65	1.62	1.61	1.62	1.65	1.52	1.52	1.55

weathering for the source areas. Generally, intense chemical weathering conditions result in the removal of labile cations (e.g. Ca^{2+}, Na^{+}, K^{+}) relative to stable residual constituents (Al^{3+}, Ti^{4+}) during weathering processes (Nesbitt & Young, 1982), due to the conversion of feldspars to clay minerals. The marine muds contain abundant mobile elements, such as Ca, Mg and K that are commonly higher than the GLOSS (Plank & Langmuir, 1998) composition (Fig. 4). Furthermore, these sediments are characterized by abundant feldspars (on average 10 % for the Neto samples and 7 % for the Crati samples; Table 1). Thus, the chemistry

https://doi.org/10.1017/S0016756814000818 Published online by Cambridge University Press

Table 3. Major- and trace-element concentrations and ratios for the studied samples from the Crati borehole

Samples	C10	C20	C30	C40	C50	C60	C70	C80	C90	C100
Oxides (wt %)										
SiO_2	46.06	46.85	46.58	46.76	46.31	46.05	46.48	46.72	45.46	45.77
TiO_2	0.81	0.83	0.83	0.78	0.79	0.78	0.77	0.78	0.77	0.75
Al_2O_3	15.64	16.34	16.24	15.57	16.02	15.19	15.43	15.59	15.14	15.09
Fe_2O_3	6.97	7.24	7.34	6.73	6.84	6.93	6.62	6.63	6.54	6.33
MnO	0.14	0.12	0.14	0.11	0.11	0.11	0.13	0.11	0.11	0.11
MgO	3.34	3.47	3.41	3.27	3.29	3.35	3.28	3.29	3.23	3.26
CaO	7.28	6.47	6.58	7.46	7.25	7.81	7.45	7.84	7.91	8.01
Na_2O	1.42	1.45	1.41	1.37	1.28	1.39	1.27	1.24	1.41	1.22
K_2O	3.06	3.01	3.02	3.08	3.19	2.91	2.99	3.05	2.98	2.95
P_2O_5	0.14	0.14	0.14	0.14	0.14	0.14	0.14	0.14	0.14	0.13
LOI	14.95	13.91	14.06	14.68	14.69	15.26	14.91	14.35	15.51	15.53
Tot.	99.81	99.83	99.75	99.95	99.91	99.92	99.47	99.74	99.20	99.15
Trace elements (ppm)										
Ni	58	61	62	55	59	60	58	59	58	57
Cr	145	139	137	135	134	131	130	139	137	140
V	182	176	180	175	178	177	174	176	179	177
Co	22	24	24	18	20	23	21	19	18	21
Cu	28	32	36	29	31	29	29	32	28	29
Zn	136	134	140	142	160	129	131	129	127	123
Nb	19	18	19	18	18	17	17	19	18	18
Ba	365	385	398	393	412	353	364	352	357	337
Rb	171	166	172	172	184	164	169	172	170	170
Sr	301	260	275	321	309	343	321	339	352	352
Y	28	30	31	28	30	29	29	28	28	28
Zr	137	156	152	142	143	140	148	139	139	135
La	53	50	60	43	49	57	55	43	58	42
Ce	91	89	87	83	87	89	90	86	90	85
Ratios										
CIA	63	64	64	63	63	63	64	65	63	64
CIA′	70	71	71	70	70	70	71	71	70	70
ICV	1.46	1.38	1.39	1.46	1.41	1.53	1.45	1.46	1.51	1.49
Samples	C110	C120	C130	C140	C150	C160	C170	C180	C190	C200
Oxides (wt %)										
SiO_2	46.99	45.69	45.68	47.61	47.28	46.46	46.77	46.90	47.30	46.38
TiO_2	0.78	0.78	0.87	0.84	0.83	0.89	0.84	0.83	0.82	0.79
Al_2O_3	15.27	15.42	17.16	16.50	16.24	17.39	16.62	17.02	16.22	15.59
Fe_2O_3	6.56	6.73	7.37	6.85	7.15	7.58	7.13	7.18	6.79	6.58
MnO	0.13	0.14	0.12	0.13	0.13	0.12	0.13	0.11	0.09	0.11
MgO	3.25	3.23	3.51	3.42	3.41	3.61	3.49	3.49	3.37	3.34
CaO	7.58	7.45	5.44	6.19	6.42	5.04	5.81	5.56	6.01	6.81
Na_2O	1.28	1.33	1.65	1.69	1.43	1.78	1.44	1.35	1.46	1.43
K_2O	2.91	3.06	3.42	3.33	2.99	3.36	3.11	3.34	3.11	3.01
P_2O_5	0.14	0.14	0.13	0.14	0.14	0.14	0.14	0.14	0.14	0.14
LOI	14.50	15.32	14.25	13.19	13.69	13.38	14.01	13.71	13.95	14.83
Tot.	99.39	99.29	99.60	99.89	99.71	99.75	99.49	99.63	99.26	99.01
Trace elements (ppm)										
Ni	59	57	59	55	60	62	62	59	60	52
Cr	141	138	145	136	138	146	139	138	141	137
V	169	176	183	165	169	185	176	179	172	174
Co	23	23	23	21	23	22	21	23	22	20
Cu	30	31	35	35	34	38	36	34	37	30
Zn	124	133	147	135	137	140	138	146	138	146
Nb	18	20	20	19	18	19	20	19	18	18
Ba	355	367	433	428	392	454	400	448	413	416
Rb	164	174	192	184	166	186	174	186	176	171
Sr	301	311	229	254	250	212	238	230	248	283
Y	30	29	30	32	33	31	32	30	32	29
Zr	150	140	147	166	157	163	166	157	163	143
La	52	37	44	46	51	59	53	55	55	50
Ce	86	88	96	93	88	97	96	101	94	94
Ratios										
CIA	64	64	64	63	65	65	65	65	65	64
CIA′	71	70	69	69	71	69	71	71	70	70
ICV	1.46	1.46	1.30	1.35	1.37	1.28	1.31	1.28	1.33	1.41

and mineralogy of the studied marine muds suggest that these sediments have been produced from source areas characterized by low–moderate weathering conditions mainly related to a temperate climate such as that occurring in the Mediterranean (e.g. Perri *et al.* 2012*b*).

Furthermore, Al/K and Rb/K ratios are also used as a broad measure of weathering, based on the contrasting mobility of these elements in the supracrustal environment (e.g. Schneider *et al.* 1997; Roy *et al.* 2008; Perri *et al.* 2014 and references therein). The Al/K ratios are low and constant (average = 4.91 ± 0.07

https://doi.org/10.1017/S0016756814000818 Published online by Cambridge University Press

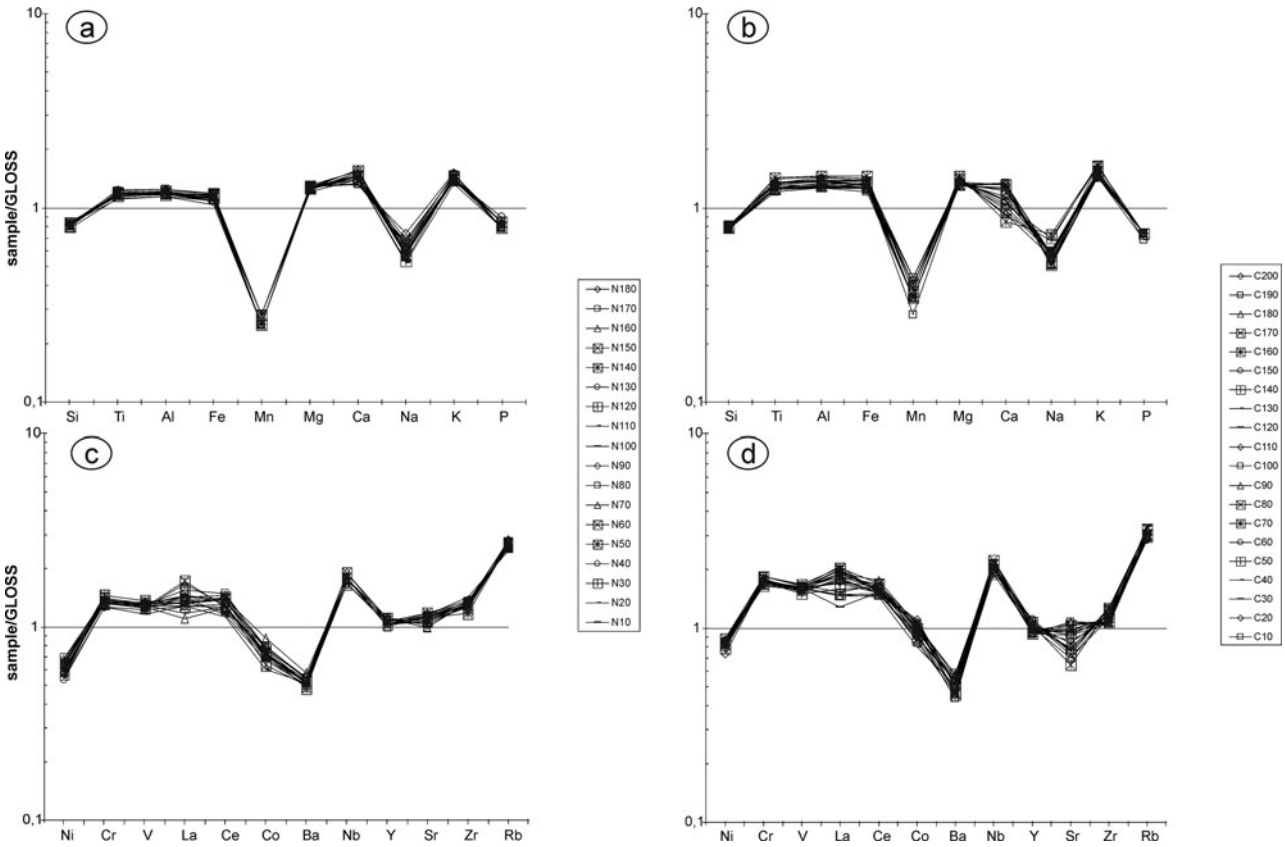

Figure 4. Major- and trace-element compositional ranges normalized to the GLOSS (Global Subducting Sediment; Plank & Langmuir, 1998).

for the Neto samples; average = 5.16 ± 0.13 for the Crati samples) for the studied muds suggesting low–moderate weathering without important fluctuations in weathering intensity. Very low and homogeneous values of Rb/K ratios (< 0.006 for both the Neto and Crati samples) are found in the studied muds, indicating low–moderate weathering in a warm–humid climate (typical of the Mediterranean area) with minimal or negligible variations over time (e.g. Mongelli *et al.* 2012; Perri *et al.* 2014 and references therein). The MFW diagram (Fig. 8; Ohta & Arai, 2007) also suggests that both the Neto and Crati sediments experienced moderate hinterland weathering.

The Index of Compositional Variability (ICV; Cox, Lowe & Cullers, 1995) uses the weight per cents of the oxides and is applied to muds as a measure of compositional maturity, with values that decrease with increasing degree of weathering. Generally, compositionally immature muds show high values of this index, tend to be found in tectonically active settings and are first-cycle deposits (van de Kamp & Leake, 1985), whereas mature muds have low ICV values and characterize tectonically quiescent or cratonic environments (Weaver, 1989) where sediment recycling is active, although they may also be produced by intense chemical weathering of first-cycle material (Barshad, 1966). All the studied muds show ICV > 1 (average = 1.60 ± 0.05 for the Neto samples; average = 1.40 ± 0.08 for the Crati samples) typical of first-cycle, compositionally immature sediments, related to tectonically active settings such as those of the Calabria–Peloritani Arc, where chemical weathering plays a minor role consistent with the medium–low CIA and CIA′ values and the trend showing in the MFW diagram.

Ternary Al_2O_3–TiO_2–Zr diagrams are used to identify the occurrence of sorting-related fractionation processes (e.g. Garcia, Coehlo & Perrin, 1991) and to discriminate mature sediments, characterized by sediment recycling and showing a wide range of ratio variations, from immature sediments, which show a more limited range of variations. Furthermore, Al/Ti ratios have also been used to give some suggestion about the source signature of fine-grained sediments, since Al and Ti exhibit low solubility during weathering and transport processes (e.g. Schieber, 1992). On the Al–Ti–Zr diagram (Fig. 9), both the Crati and Neto muds studied are clustered in the centre of the plot with a limited range of TiO_2/Zr variations, suggesting poor sorting and recycling and rapid deposition of the sediments. This trend indicates that the studied muds are compositionally immature, according to their ICV values previously mentioned. On the Al–Ti–Zr diagram (Fig. 9) the starting points of the recycling trends are different for the Neto and Crati sediments; this indicates that the parent materials of the Neto and Crati sediments prior to the recycling process were different. Furthermore, the 90 % confidence regions of the Neto and Crati sediments do not overlap. Therefore,

https://doi.org/10.1017/S0016756814000818 Published online by Cambridge University Press

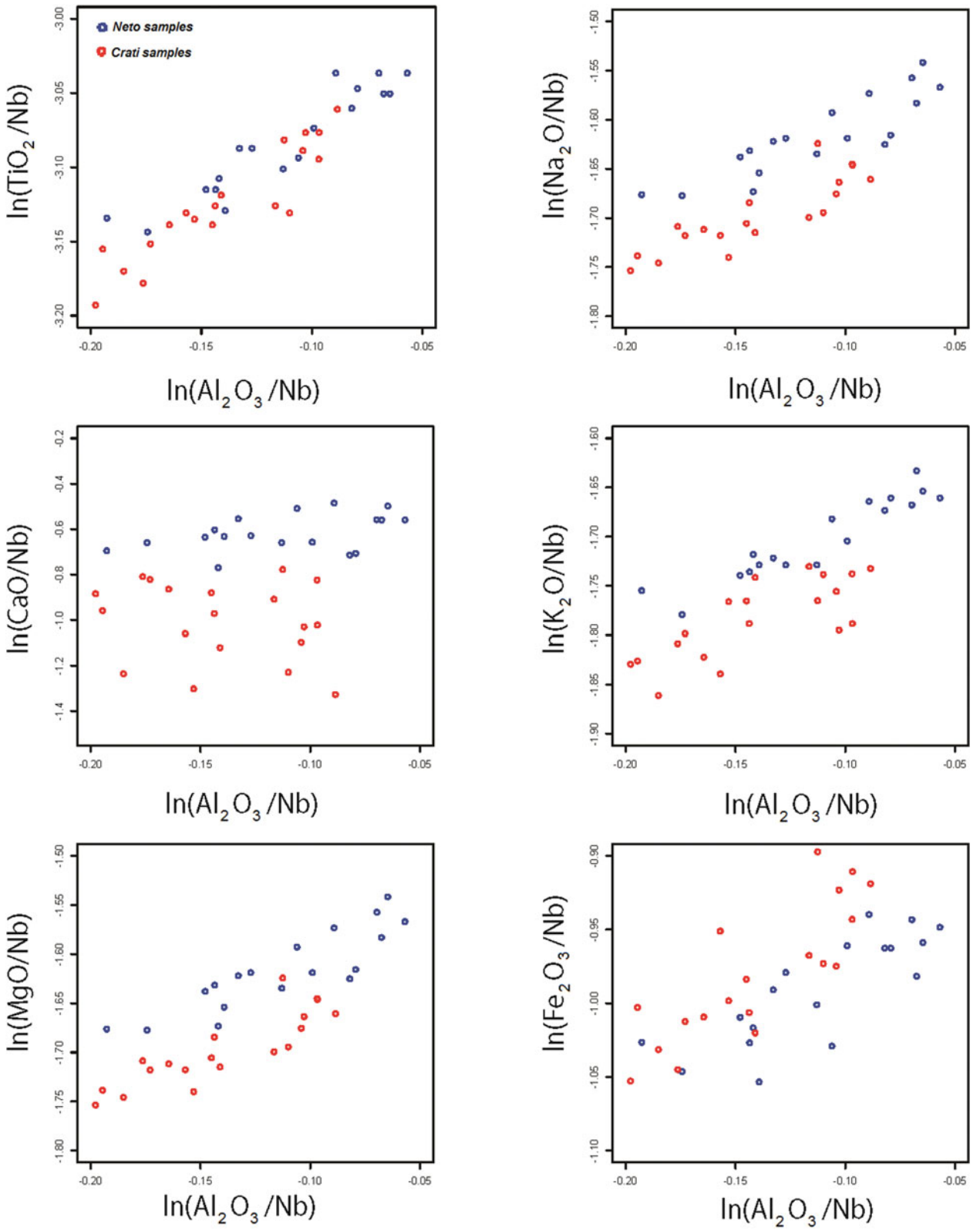

Figure 5. (Colour online) Variation diagrams using major- and trace-element ratios for the Neto and Crati muds.

the parent populations of these borehole sediments are different at the 90 % significance level.

5.b. Provenance signatures

The Crati muds show higher Ti, Al, Fe, Mg and K values than the Neto samples and some variations in CaO and Sr contents as well as in carbonate mineral (calcite and dolomite) contents (Fig. 10). This composition reflects a multi-cyclic provenance from recycled Mesozoic to Tertiary extrabasinal carbonates of the Pollino Massif and, thus, carbonate strata of the other tectono-stratigraphic units of the southern Apennine fold-thrust belt, and from plutonic and metamorphic rocks of the

https://doi.org/10.1017/S0016756814000818 Published online by Cambridge University Press

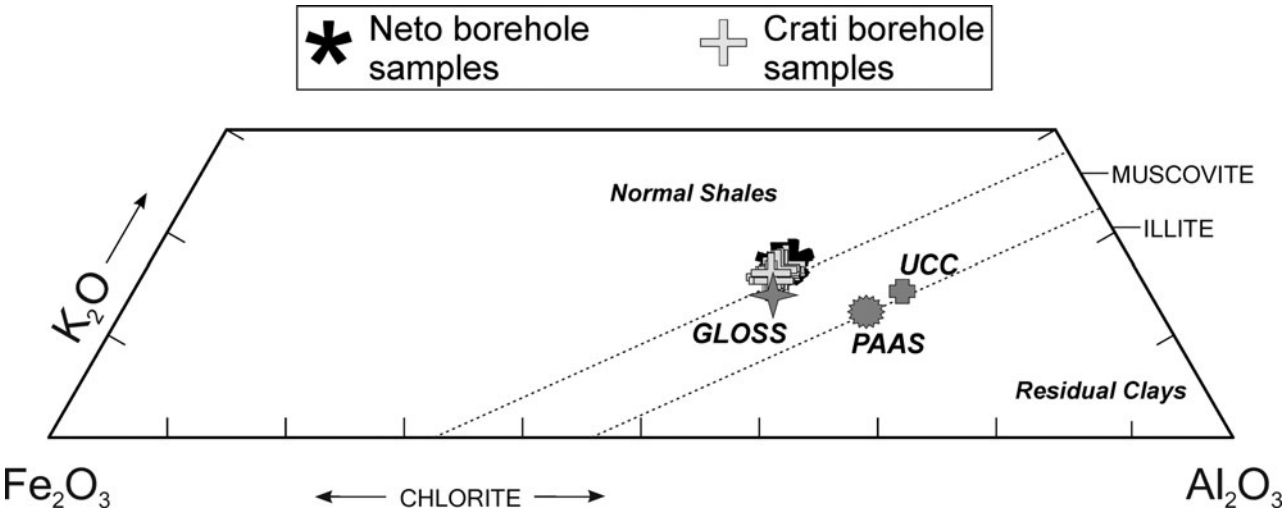

Figure 6. Fe_2O_3–K_2O–Al_2O_3 diagram where the studied muds plot along a trend defined by chlorite and muscovite–illite end-members. GLOSS – Global Subducting Sediment; PASS – Post-Archaean Australian Shale; UCC – Upper Continental Crust.

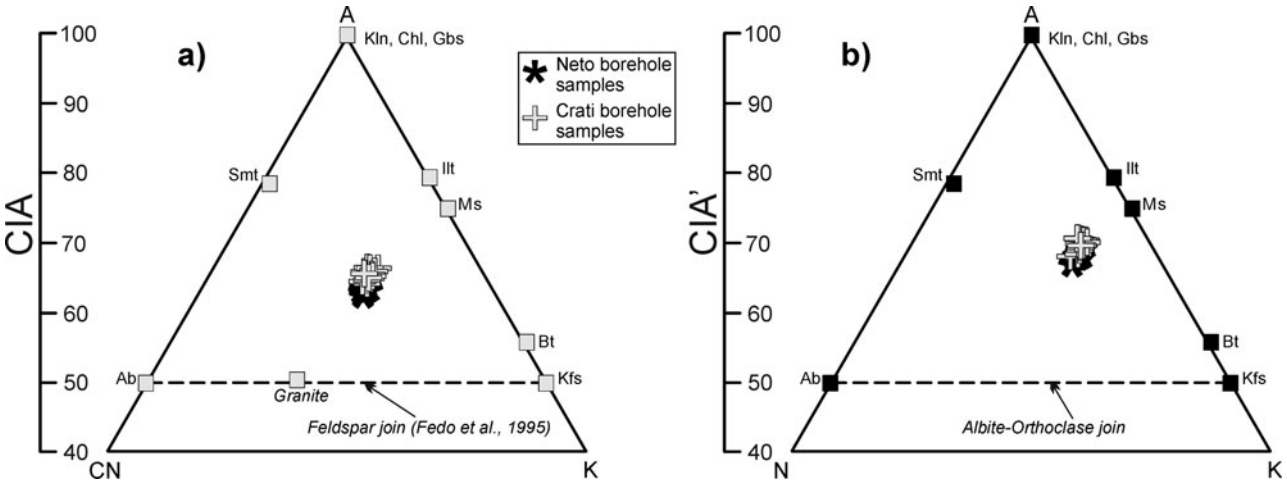

Figure 7. (a) Ternary A–CN–K (Fedo *et al.* 1995) and (b) A–N–K diagrams. Legend: Ms – muscovite; Ilt – illite; Kln – kaolinite; Chl –chlorite; Gbs – gibbsite; Smt – smectite; Bt – biotite; Pl – plagioclase; Kfs – K-feldspar; A – Al_2O_3; CN – CaO + Na_2O; K – K_2O; CIA – Chemical Index of Alteration (Nesbitt & Young, 1982).

Sila Massif (e.g. Critelli & Le Pera, 2003; Perri *et al.* 2012*b*). On the other hand, the Neto muds mainly show high percentages of CaO and Sr as well as high percentages of carbonate minerals (calcite and dolomite) (Fig. 10), with lower Ti, Al, Fe, Mg and K values than the Crati samples. These contents are mainly related to provenance from the Neogene–Quaternary carbonate-rich marine deposits of the Crotone Basin (e.g. Barone *et al.* 2008; Zecchin *et al.* 2013; Perri *et al.* 2014; Perri, Dominici & Critelli, 2014), which mostly influences the composition of the Neto marine muds, with subordinate sedimentary and metasedimentary source rocks, and plutonic–metamorphic rocks from the Sila Massif (e.g. Perri *et al.* 2012*b*). In particular, samples from the upper portion of the Crati borehole (from C10 to C120) contain higher percentages of CaO, Sr and carbonate minerals (calcite and dolomite) than the samples from the lower portion. These variations in carbonate supply suggest major contributions, in the upper portion of the borehole, from Mesozoic–Cenozoic carbonate rocks of the southeastern flank of the Pollino Massif. The Neto borehole samples show quite homogeneous values of CaO, Sr and carbonate minerals (calcite and dolomite) testifying to a mixed source from carbonates of the Neogene–Quaternary marine deposits of the Crotone Basin with subordinate siliciclastic sedimentary, metasedimentary and plutonic–metamorphic source rocks from the Sila Massif.

Table 4 shows the results of the Mann–Whitney U-test conducted on some incompatible (Y, Zr and Nb) against compatible element (Ni, V and Cr) log-ratios. All three log-ratios identified statistically significant differences between the Neto and Crati samples, and the Crati samples are always enriched in compatible elements. The discriminant diagram of Roser & Korsch (1988) suggests that both the Neto and Crati sediments are related to a recycled and reworked orogen, but the Crati sediments are more dislocated towards a mafic source domain (Fig. 11). In addition, the Neto and Crati sediments depict different weathering trends on

https://doi.org/10.1017/S0016756814000818 Published online by Cambridge University Press

Table 4. Mann–Whitney U-test of incompatible and compatible trace-element log-ratios

	Median of Neto samples	Median of Crati samples	*p*-values*
ln(Y/Ni)	− 0.307	− 0.682	**< 0.00001**
ln(Zr/V)	0.202	− 0.183	**< 0.00001**
ln(Nb/Cr)	− 1.910	− 2.030	**< 0.00001**

*Statistically significant *p*-values are marked in bold

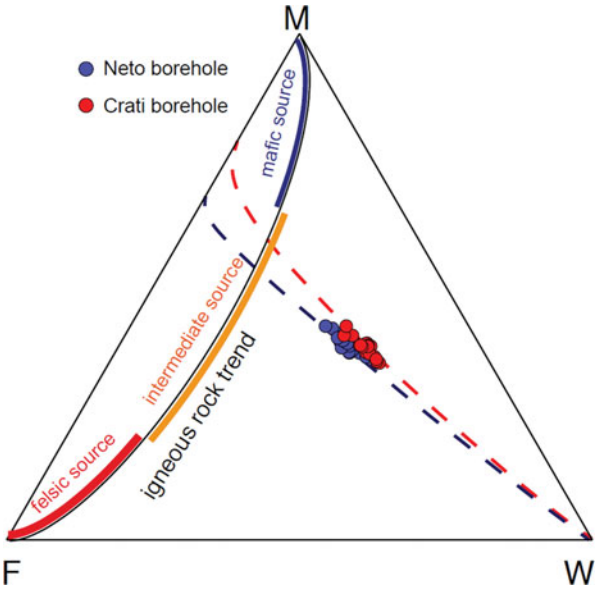

Figure 8. (Colour online) The MFW diagram (Ohta & Arai, 2007) suggesting moderate weathering conditions. M – mafic source; F – felsic source; W – weathered material. The weathering trends of both the Neto and Crati sediments indicate an intermediate source-rock composition; however, the weathering trends suggest a relatively mafic composition for the Crati sediments. Compositional linear trends were drawn following the method of von Eynatten (2004).

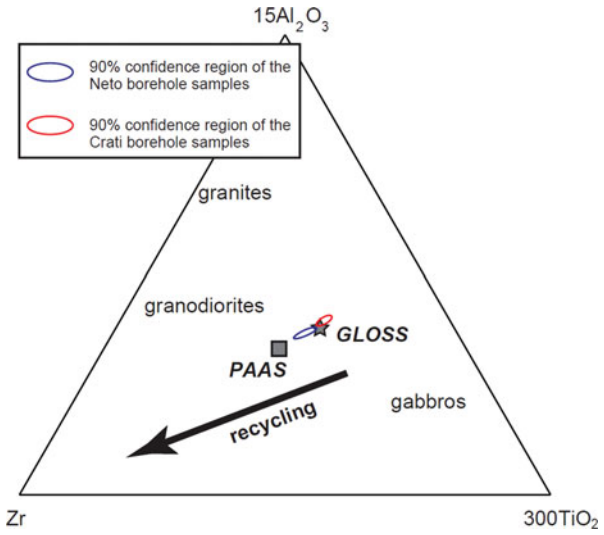

Figure 9. (Colour online) Ternary $15Al_2O_3$–$300TiO_2$–Zr plot (modified from Garcia, Coehlo & Perrin, 1991) showing the confidence regions of the studied muds. 90 % confidence regions were drawn following the method of Weltje (2002). GLOSS – Global Subducting Sediment; PAAS – Post-Archaean Australian Shale.

the MFW diagram, and the source-rock composition for the Crati sediments indicates a more mafic source composition compared to the Neto sediments (Fig. 8). All these facts suggest that the hinterland composition of the Crati drainage area was on average more mafic in composition than the Neto drainage area.

Different provenance proxies, including triangular relationships of V–Ni–La*4 (e.g. Perri, Muto & Belviso, 2011), have been commonly used to evaluate the source area(s) composition. The V–Ni–La*4 ternary diagram shows the fields representative of felsic, mafic and ultramafic rocks plot separately (e.g. Bracciali *et al.* 2007; Perri, Muto & Belviso, 2011) and shows the fields of the main tectonic units of the northern Calabria–Peloritani Arc (Fig. 12); the studied muds plot close to the felsic composition and also to the compositions of the main units of the northern Calabria–Peloritani Arc, with the Crati sediments being slightly dislocated towards a mafic source domain (Fig. 12). Thus, the Crati drainage area is on average more mafic in composition than the Neto drainage area, according to the previous considerations. The studied samples show higher Fe content compared to the global average Fe content of riverine sediments (4.81 ± 0.19 wt %; Poulton & Raiswell, 2002). In particular, the Crati samples have higher Fe content than the Neto samples; the high Fe content in the Crati muds can be related to some contribution from the Fe-rich mafic source rocks in the catchment area.

The higher mafic concentration of the Crati mud samples is probably related to the Malvito, Diamante–Terranova and Gimigliano Ophiolitiferous units (see Fig. 1) that are exposed in the Crati drainage basin (e.g. Critelli & Le Pera, 1995, 2003).

High Al concentrations in sediments compared to those of the UCC (McLennan, Taylor & Hemming, 2006) is indicative of high detrital input. In particular, the Crati muds show higher Al contents than the Neto muds; this distribution may be attributed to the higher erosion rates of the Crati River drainage system than those of the Neto River drainage system, since a general increase in the concentration of Al is frequently indicative of high erosion rates (e.g. Karbassi & Amirnezhad, 2004; Perri *et al.* 2012*b*).

For the discrimination of island and continental arc, within-plate (continental rift and ocean island together) and collisional tectonic settings, a new diagram obtained from linear discriminant analysis of natural logarithm transformed ratios of major and trace elements has been used (Fig. 13) (e.g. Verma *et al.* 2013). This

https://doi.org/10.1017/S0016756814000818 Published online by Cambridge University Press

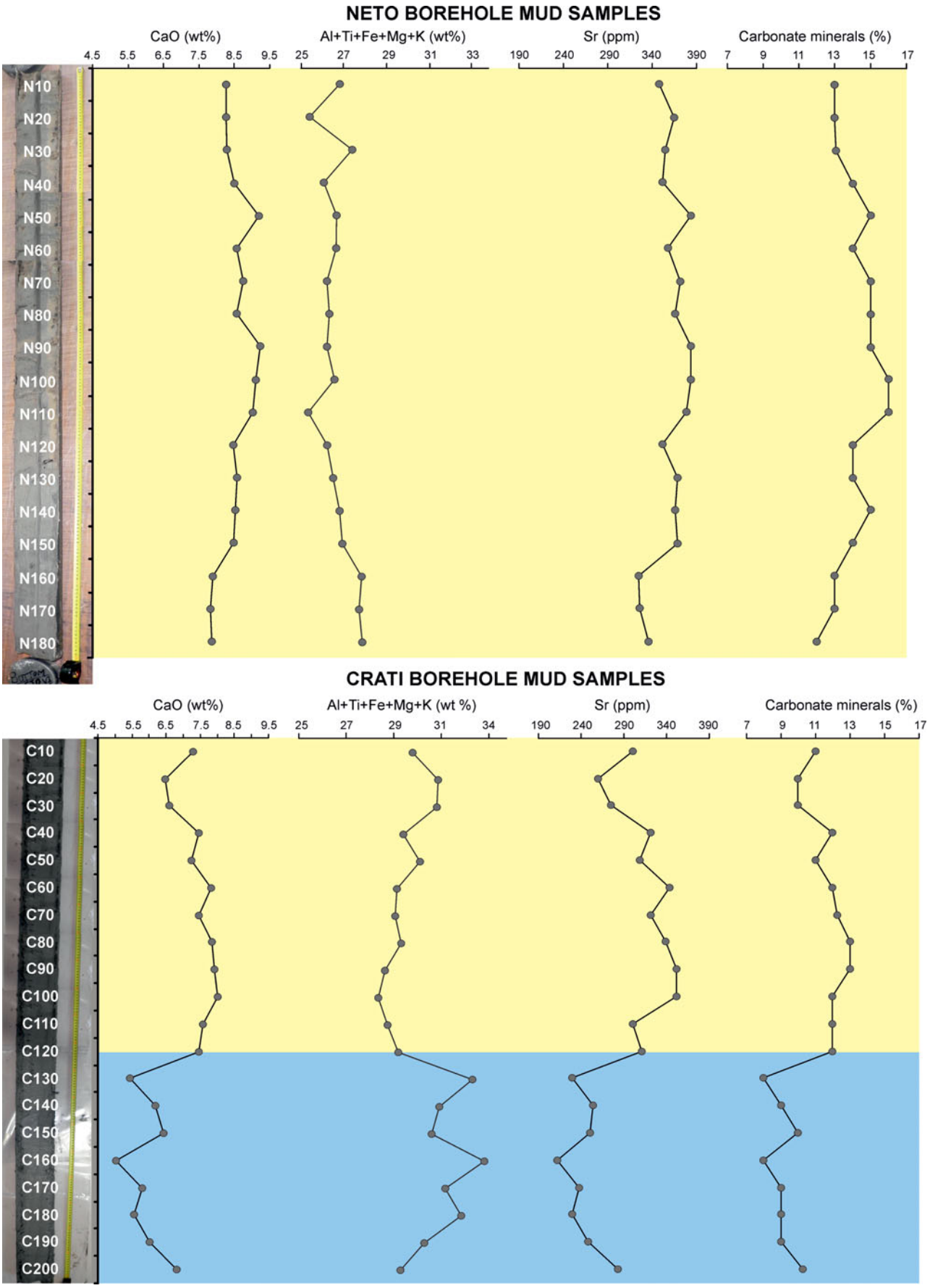

Figure 10. (Colour online) Main chemical and mineralogical variations through the samples from the Neto and Crati boreholes.

https://doi.org/10.1017/S0016756814000818 Published online by Cambridge University Press

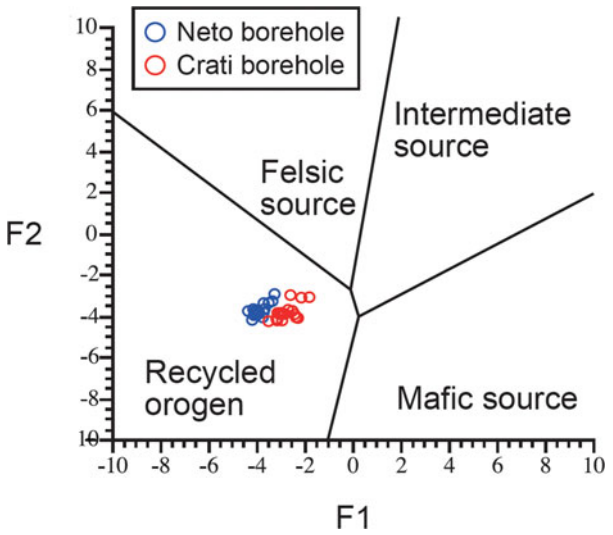

Figure 11. (Colour online) Discriminant diagram of Roser & Korsch (1988) suggesting that the studied sediments are related to a recycled orogen. F1 and F2 are discriminant functions using the chemical composition of the studied samples.

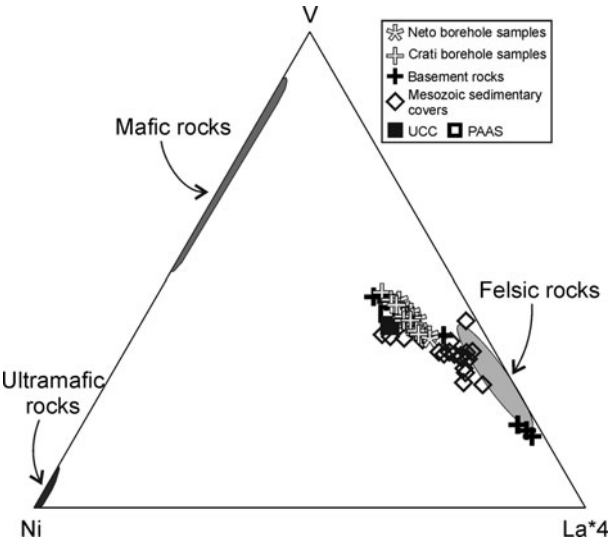

Figure 12. V–Ni–La*4 ternary diagram, showing fields representative of felsic, mafic and ultramafic rocks plot separately (e.g. Bracciali *et al.* 2007; Perri, Muto & Belviso, 2011). The studied samples plot close to the felsic composition and to the Palaeozoic basement rocks and Mesozoic sedimentary covers. UCC – Upper Continental Crust; PAAS – Post-Archaean Australian Shale.

diagram indicates that the studied samples are related to a collisional setting (Fig. 13).

6. Concluding remarks

The Ionian coast of the Calabrian region represents an excellent area to study the relationships between source areas and deep-marine basins, using the mineralogical and chemical compositional signatures of marine muds. The northern Ionian Basin is mainly characterized by two submarine fans, the Crati, to the north, and the Neto, to the south, related to the Crati and Neto river fluvial systems, coupled to diverse smaller coastal

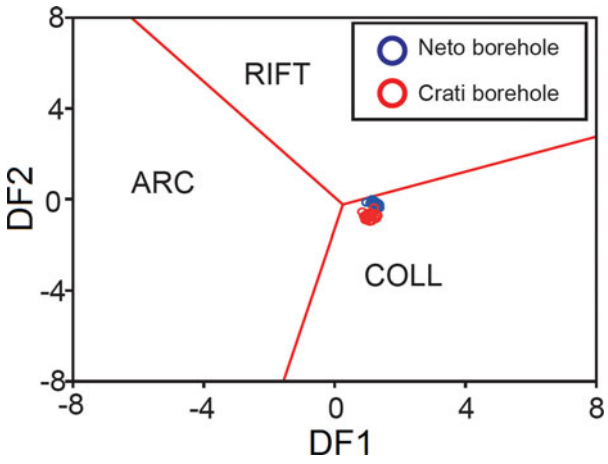

Figure 13. (Colour online) Diagram of the tectonic settings (modified from Verma *et al.* 2013). ARC – island and continental arc; RIFT – within-plate (continental rift and ocean island together); COLL – collisional setting. DF1 and DF2 are discriminant functions using the chemical composition of the studied samples.

rivers, draining the southern Apennines thrust belt (i.e. Pollino Massif), the Calabria continental block (i.e. Sila Massif) and the Plio-Pleistocene marine deposits of the Crotone Peninsula, from north to south.

The deep-marine muds, collected from the Crati II and the Neto VI boreholes, show a similar mineralogical distribution, dominated by phyllosilicates over quartz, carbonates (calcite and dolomite) and feldspars (plagioclase and K-feldspar). The geochemical proxies of the studied muds, based on the V–Ni–La*4 and other discriminant diagrams and some incompatible/compatible element ratios, mainly reflect a provenance characterized by felsic rocks with minor mafic–ultramafic supply. In particular, the hinterland composition of the Crati drainage area is on average more mafic in composition than the Neto drainage area. A significant variation in the carbonate input is further recorded, mostly for the Crati muds. The values of the CIA and CIA′ indices and the trend showing in the MFW diagram, suggest low–moderate source area weathering. The low and constant Al/K and Rb/K ratios further suggest low–moderate weathering conditions without important fluctuations in weathering intensity. The ICV values and the distribution of both the Crati and Neto muds on the Al_2O_3–TiO_2–Zr ternary diagram indicate that the studied samples are first-cycle, compositionally immature sediments, related to tectonically active (collision) settings such as those of the Calabria–Peloritani Arc, where chemical weathering plays a minor role.

Acknowledgements. This research has been carried out within the OGS funded projects WGDT (Morphology and Architecture of the Western Portions of the Gulf of Taranto: A Study of Submarine Instability in a Tectonically Active Margin; Resp. S. Critelli), and MIUR-UNICAL (Relationships between Tectonic Accretion, Volcanism and Clastic Sedimentation within the Circum-Mediterranean Orogenic Belts, 2006–2011; Resp. S. Critelli). The authors are grateful to Tohru Ohta for his help and contribution to the

https://doi.org/10.1017/S0016756814000818 Published online by Cambridge University Press

statistical tests and analyses of the compositional data and for reviewing an early version of the manuscript. The authors are indebted to Gert Jan Weltje and the Editor Juergen Schieber for their reviews and suggestions on the final version of the manuscript.

References

AITCHISON, J. 1986. *Statistical Analysis of Compositional Data*. London: Chapman & Hall, 416 pp.

BARONE, M., CRITELLI, S., DOMINICI, R. & MUTO, F. 2008. Detrital modes in a late Miocene wedge-top basin, northeastern Calabria, Italy: compositional record of wedge-top partitioning. *Journal of Sedimentary Research* **78**, 693–711.

BARSHAD, I. 1966. The effect of a variation in precipitation on the nature of clay mineral formation in soils from acid and basic igneous rocks. In *Proceedings of the International Clay Conference* (eds L. Heller & A. Weiss), pp. 167–73. Jerusalem: Israel Programme of Scientific Translation.

BAULUZ, B., MAYAYO, M. J., FERNANDEZ-NIETO, C. & GONZALEZ LOPEZ, J. M. 2000. Geochemistry of Precambrian and Paleozoic siliciclastic rocks from the Iberian Range (NE Spain): implications for source-area weathering, sorting, provenance, and tectonic setting. *Chemical Geology* **168**, 135–50.

BONARDI, G., CAVAZZA, W., PERRONE, V. & ROSSI, S. 2001. Calabria-Peloritani Terrane and Northern Ionian Sea. In *Anatomy of an Orogen: The Apennines and Adjacent Mediterranean Basins* (eds G. B. Vai & I. P. Martini), pp. 287–306. Dordrecht/Boston/London: Kluwer Academic Publishers.

BRACCIALI, L., MARRONI, M., PANDOLFI, L. & ROCCHI, S. 2007. Geochemistry and petrography of Western Tethys Cretaceous sedimentary covers (Corsica and Northern Apennines): from source areas to configuration of margins. In *Sedimentary Provenance and Petrogenesis: Perspectives from Petrography and Geochemistry* (eds J. Arribas, S. Critelli & M. J. Johnsson), pp. 73–93. Geological Society of America Special Paper 420.

CAVALCANTE, F., FIORE, S., LETTINO, A., PICCARRETA, G. & TATEO, F. 2007. Illite-smectite mixed layers in sicilide shales and piggy-back deposits of the Gorgoglione Formation (Southern Apeninnes): geological inferences geodynamic implications. *Bollettino della Società Geologica Italiana* **126**, 241–54.

CAVAZZA, W. & INGERSOLL, R. V. 2005. Detrital modes of the Ionian forearc basin fill (Oligocene–Quaternary) reflect the tectonic evolution of the Calabria–Peloritani terrane (southern Italy). *Journal of Sedimentary Research* **75**, 268–379.

CERAMICOLA, S., PRAEG, D., COSTE, M., FORLIN, E., COVA, A., COLIZZA, E. & CRITELLI, S. 2014. Submarine mass-movements along the slopes of the active Ionian continental margins and their consequences for marine geohazards (Mediterranean Sea). In *Submarine Mass Movements and Their Consequences, Advances in Natural and Technological Hazards Research 37* (eds S. Krastel *et al.*), pp. 295–306. Dordrecht: Springer International Publishing.

CORBI, F., FUBELLI, G., LUCÀ, F., MUTO, F., PELLE, T., ROBUSTELLI, G., SCARCIGLIA, F. & DRAMIS, F. 2009. Vertical movements in the Ionian margin of the Sila Massif (Calabria, Italy). *Bollettino della Societa Geologica Italiana* **128**, 731–8.

COX, R., LOWE, D. R. & CULLERS, R. L. 1995. The influence of sediment recycling and basement composition on evolution of mud rock chemistry in the southwestern United States. *Geochimica et Cosmochimica Acta* **59**, 2919–40.

CRICHTON, J. G. & CONDIE, K. C. 1993. Trace elements as source indicators in cratonic sediments: a case study from the Early Proterozoic Libby Creek Group, southeastern Wyoming. *Journal of Geology* **101**, 319–32.

CRITELLI, S., DOMINICI, R., MUTO, F., PERRI, F. & TRIPODI, V. 2012. Composition and depositional architecture of late Quaternary sediments in the deep-water northern Ionian Basin, southern Italy. *Rendiconti Online della Società Geologica Italiana* **21**, 959–61.

CRITELLI, S. & LE PERA, E. 1995. Tectonic evolution of the Southern Apennines thrust-belt (Italy) as reflected in modal compositions of Cenozoic sandstone. *Journal of Geology* **103**, 95–105.

CRITELLI, S. & LE PERA, E. 1998. Post-Oligocene sediment dispersal systems and unroofing history of the Calabrian Microplate, Italy. *International Geology Review* **48**, 609–37.

CRITELLI, S. & LE PERA, E. 2003. Provenance relations and modern sand petrofacies in an uplifted thrust-belt, northern Calabria, Italy. In *Quantitative Provenance Studies in Italy* (eds R. Valloni & A. Basu), pp. 25–39. Servizio Geologico Nazionale, Memorie Descrittive della Carta Geologica d'Italia, vol. 61.

CRITELLI, S., LE PERA, E., GALLUZZO, F., MILLI, S., MOSCATELLI, M., PERROTTA, S. & SANTANTONIO, M. 2007. Interpreting siliciclastic-carbonate detrital modes in foreland basin systems: an example from Upper Miocene arenites of the Central Apennines, Italy. In *Sedimentary Provenance: Petrographic and Geochemical Perspectives* (eds J. Arribas, S. Critelli & M. Johnsson), pp. 107–33. Geological Society of America Special Paper 420.

CRITELLI, S., MONGELLI, G., PERRI, F., MARTIN-ALGARRA, A., MARTIN-MARTIN, M., PERRONE, V., DOMINICI, R., SONNINO, M. & ZAGHLOUL, M. N. 2008. Compositional and geochemical signatures for the sedimentary evolution of the Middle Triassic–Lower Jurassic continental redbeds from western-central Mediterranean Alpine chains. *Journal of Geology* **116**, 375–86.

CRITELLI, S., MUTO, F., TRIPODI, V. & PERRI, F. 2013. Link between thrust tectonics and sedimentation processes of stratigraphic sequences from the southern Apennines foreland basin system, Italy. *Rendiconti Online della Società Geologica Italiana* **25**, 21–42.

FEDO, C. M., NESBITT, H. W. & YOUNG, G. M. 1995. Unraveling the effect of potassium metasomatism in sedimentary rocks and paleosols, with implications for paleoweathering conditions and provenance. *Geology* **23**, 921–4.

GARCIA, D., COEHLO, J. & PERRIN, M. 1991. Fractionation between TiO_2 and Zr as a measure of sorting within shale and sandstone series (northern Portugal). *European Journal of Mineralogy* **3**, 401–14.

HERRON, M. M. 1988. Geochemical classification of terrigenous sands and shales from core or log data. *Journal of Sedimentary Petrology* **58**, 820–9.

KARBASSI, A. R. & AMIRNEZHAD, R. 2004. Geochemistry of heavy metals and sedimentation rate in a bay adjacent to the Caspian Sea. *International Journal of Environmental Science and Technology* **1**, 199–206.

KNOTT, S. D. & TURCO, E. 1991. Late Cenozoic kinematics of the Calabrian Arc, southern Italy. *Tectonics* **10**, 1164–72.

KRUMM, S. 1996. WINFIT 1.2: version of November 1996 (The Erlangen geological and mineralogical software collection) of "WINFIT 1.0: a public domain program for interactive profile-analysis under WINDOWS". XIII Conference on Clay Mineralogy and Petrology, Praha, 1994. *Acta Univers itatis Carolinae Geologica* **38**, 253–61.

LE PERA, E., ARRIBAS, J., CRITELLI, S. & TORTOSA, A. 2001. The effects of source rocks and chemical weathering on the petrogenesis of siliciclastic sand from the Neto River (Calabria, Italy): implications for provenance studies. *Sedimentology* **48**, 357–77.

LUGLI, S., DOMINICI, R., BARONE, M., COSTA, E. & CAVOZZI, C. 2007. Messinian halite and residual facies in the Crotone basin (Calabria, Italy). In *Evaporites Through Space and Time* (eds B. C. Schreiber, S. Lugli & M. Baçbel), pp. 169–78. Geological Society of London, Special Publication no. 285.

MCLENNAN, S. M., TAYLOR, S. R. & HEMMING, S. R. 2006. Composition, differentiation, and evolution of continental crust: constrains from sedimentary rocks and heat flow. In *Evolution and Differentiation of the Continental Crust* (eds M. Brown & T. Rushmer), pp. 92–134. Cambridge: Cambridge University Press.

MONGELLI, G., CRITELLI, S., PERRI, F., SONNINO, M. & PERRONE, V. 2006. Sedimentary recycling, provenance and paleoweathering from chemistry and mineralogy of Mesozoic continental redbed mudrocks, Peloritani Mountains, Southern Italy. *Geochemical Journal* **40**, 197–209.

NESBITT, H. W. & YOUNG, G. M. 1982. Early Proterozoic climates and plate motions inferred from major element chemistry of lutites. *Nature* **299**, 715–7.

OHTA, T. & ARAI, H. 2007. Statistical empirical index of chemical weathering in igneous rocks: a new tool for evaluating the degree of weathering. *Chemical Geology* **240**, 280–97.

PERRI, F. 2008. Clay mineral assemblage of the Middle Triassic-Lower Jurassic mudrocks from western-central Mediterranean Alpine chains. *Periodico di Mineralogia* **77**, 23–40.

PERRI, F., BORRELLI, L., CRITELLI, S. & GULLÀ, G. 2014. Chemical and minero-petrographic features of Plio-Pleistocene fine-grained sediments in Calabria (southern Italy). *Italian Journal of Geosciences* **133**, 101–15.

PERRI, F., CIRRINCIONE, R., CRITELLI, S., MAZZOLENI, P. & PAPPALARDO, A. 2008. Clay mineral assemblages and sandstone compositions of the Mesozoic Longobucco Group (north-eastern Calabria): implication for burial history and diagenetic evolution. *International Geology Review* **50**, 1116–31.

PERRI, F., CRITELLI, S., CAVALCANTE, F., MONGELLI, G., DOMINICI, R., SONNINO, M. & DE ROSA, R. 2012*a*. Provenance signatures for the Miocene volcaniclastic succession of the Tufiti di Tusa Formation, southern Apennines, Italy. *Geological Magazine* **149**, 423–42.

PERRI, F., CRITELLI, S., DOMINICI, R., MUTO, F., TRIPODI, V. & CERAMICOLA, S. 2012*b*. Provenance and accommodation pathways of late Quaternary sediments in the deep-water northern Ionian Basin, southern Italy. *Sedimentary Geology* **280**, 244–59.

PERRI, F., CRITELLI, S., MARTÌN-ALGARRA, A., MARTÌN-MARTÌN, M., PERRONE, V., MONGELLI, G. & ZATTIN, M. 2013. Triassic redbeds in the Malaguide Complex (Betic Cordillera – Spain): petrography, geochemistry, and geodynamic implications. *Earth-Science Reviews* **117**, 1–28.

PERRI, F., CRITELLI, S., MONGELLI, G. & CULLERS, R. L. 2011. Sedimentary evolution of the Mesozoic continental redbeds using geochemical and mineralogical tools: the case of Upper Triassic to Lowermost Jurassic M.te di Gioiosa mudstones (Sicily, Southern Italy). *International Journal of Earth Sciences* **100**, 1569–87.

PERRI, F., DOMINICI, R. & CRITELLI, S. 2014. Stratigraphy, composition and provenance of argillaceous marls from the Calcare di Base Formation, Rossano Basin (northeastern Calabria). *Geological Magazine*. Published online 15 April 2014. doi: 0.1017/S0016756814000089

PERRI, F., GRECO, A., ALDEGA, L., CORRADO, S., CRITELLI, S. & DI PAOLO, L. 2012*c*. Composition, provenance and thermal history of sedimentary successions from the Cilento Group (southern Apennines). *Rendiconti Online della Società Geologica Italiana* **21**, 203–5.

PERRI, F., MUTO, F. & BELVISO, C. 2011. Links between composition and provenance of Mesozoic siliciclastic sediments from Western Calabria (Southern Italy). *Italian Journal of Geosciences* **130**, 318–29.

PERRI, F. & OTHA, T. 2014. Paleoclimatic conditions and paleoweathering processes on Mesozoic continental redbeds from western-central Mediterranean Alpine chains. *Palaeogeography, Palaeoclimatology, Palaeoecology* **395**, 144–57.

PLANK, T. & LANGMUIR, C. H. 1998. The chemical composition of subducting sediment and its consequences for the crust and mantle. *Chemical Geology* **145**, 325–94.

POULTON, S. W. & RAISWELL, R. 2002. The low-temperature geochemical cycle of iron: from continental fluxes to marine sediment deposition. *American Journal of Science* **302**, 774–805.

POTTER, P. E. 1978, Petrology and chemistry of modern big river sands. *Journal of Geology* **86**, 423–49.

REBESCO, M., NEAGU, R. C., CUPPARI, A., MUTO, F., ACCETTELLA, D., DOMINICI, R., COVA, A., ROMANO, C. & CABURLOTTO, A. 2009. Morphobathymetric analysis and evidence of submarine mass movements in the western Gulf of Taranto (Calabria margin, Ionian Sea). *International Journal of Earth Sciences* **4**, 791–805.

ROBUSTELLI, G., LUCÀ, F., CORBI, F., PELLE, T., DRAMIS, F., FUBELLI, G., SCARCIGLIA, F., MUTO, F. & CUGLIARI, D. 2009. Alluvial terraces on the Ionian coast of northern Calabria, southern Italy: implications for tectonic and sea level controls. *Geomorphology* **106**, 165–79.

ROMAGNOLI, C. & GABBIANELLI, G. 1990. Late Quaternary sedimentation and soft-sediment deformations in the Corigliano Basin (Gulf of Taranto, northern Ionian Sea). *Giornale di Geologia* **52**, 33–53.

ROSER, B. & KORSCH, R. 1988. Provenance signatures of sandstone-mudstone suites determined using discriminant function analysis of major-element data. *Chemical Geology* **67**, 119–39.

ROSSI, S. & SARTORI, R. 1981. A seismic reflection study of the External Calabrian Arc in the Northern Ionian Sea (Eastern Mediterranean). *Marine Geophisical Researches* **4**, 403–26.

ROY, P. D., CABALLERO, M., LOZANO, R. & SMYTATZ-KLOSS, W. 2008. Geochemistry of late Quaternary sediments from Tecomuco lake, central Mexico: implication to chemical weathering and provenance. *Chemie der Erde* **68**, 383–93.

SCARCIGLIA, F., LE PERA, E. & CRITELLI, S. 2007. The onset of sedimentary cycle in a mid-latitude upland environment: weathering, pedogenesis and geomorphic processes on plutonic rocks (Sila Massif, Calabria). In *Sedimentary Provenance: Petrographic and Geochemical Perspectives* (eds J. Arribas, S. Critelli & M. Johnsson),

pp. 149–66. Geological Society of America Special Paper 420.

SCHIEBER, J. 1992. A combined petrographical–geochemical provenance study of the Newland Formation, Mid-Proterozoic of Montana. *Geological Magazine* **129**, 223–37.

SCHNEIDER, R. R., PRICE, B., MÜLLER, P. J., KROON, D. & ALEXANDER, I. 1997. Monsoon-related variations in Zaire (Congo) sediment load and influence of fluvial silicate supply on marine productivity in the east equatorial Atlantic during the last 200,000 years. *Paleoceanography*, **12**, 463–81.

SPERANZA, F., MINELLI, L., PIGNATELLI, A. & CHIAPPINI, M. 2012. The Ionian Sea: the oldest in situ ocean fragment of the world? *Journal of Geophysical Research* **117**, B12101.

TRIPODI, V., MUTO, F. & CRITELLI, S. 2013. Structural style and tectonostratigraphic evolution of the Neogene-Quaternary Siderno Basin, southern Calabrian Arc, Italy. *International Geology Review* **55**, 468–81.

VAN DE KAMP, P. C. & LEAKE, B. E. 1985. Petrography and geochemistry of feldspathic and mafic sediments of the Northeastern Pacific Margin. *Transactions of the Royal Society of Edinburgh: Earth Sciences* **76**, 411–49.

VAN DIJK, J. P., BELLO, M., BRANCALEONI, G. P., CANTARELLA, G., COSTA, V., FRIXA, A., GOLFETTO, F., MERLINI, S., RIVA, M., TORRICELLI, S., TOSCANO, C. & ZERILLI, A., 2000. A regional structural model for the northern sector of the Calabria Arc (Southern Italy). *Tectonophysics* **324**, 267–320.

VERMA, S. P., PANDARINATH, K., VERMA, S. K. & AGRAWAL, S. 2013. Fifteen new discriminant-function-based multi-dimensional robust diagrams for acid rocks and their application to Precambrian rocks. *Lithos* **168–169**, 113–23.

Von EYNATTEN, H. 2004. Statistical modelling of compositional trends in sediments. *Sedimentary Geology* **171**, 79–89.

WEAVER, C. E. 1989. *Clays, Muds, and Shales.* Developments in Sedimentology, 44. Amsterdam: Elsevier, 819 pp.

WELTJE, G. T. 2002. Quantitative analysis of detrital modes: statistically rigorous confidence regions in ternary diagrams and their use in sedimentary petrology. *Earth-Science Reviews* **57**, 211–53.

WRONKIEWICZ, D. J. & CONDIE, K. C. 1987. Geochemistry of Archean shales from the Witwatersrand Supergroup, South Africa: source-area weathering and provenance. *Geochimica et Cosmochimica Acta* **51**, 2401–16.

ZAGHLOUL, M. N., CRITELLI, S., PERRI, F., MONGELLI, G., PERRONE, V., SONNINO, M., TUCKER, M., AIELLO, M. & VENTIMIGLIA, C. 2010. Depositional systems, composition and geochemistry of Triassic rifted continental margin redbeds of Internal Rif Chain, Morocco. *Sedimentology* **57**, 312–50.

ZECCHIN, M., CERAMICOLA, S., GORDINI, E., DEPONTE, M. & CRITELLI, S. 2011. Cliff overstep model and variability in the geometry of transgressive erosional surfaces in high-gradient shelves: the case of the Ionian Calabrian margin (southern Italy). *Marine Geology* **281**, 43–58.

ZECCHIN, M., CIVILE, D., CAFFAU, M., MUTO, F., DI STEFANO, A. & MANISCALCO, R., CRITELLI, S. 2013. The Messinian succession of the Crotone Basin (southern Italy) I: stratigraphic architecture reconstructed by seismic and well data. *Marine and Petroleum Geology* **48**, 455–73.